Thin Solid Films 548 (2013) 551–555

Contents lists available at ScienceDirect

Thin Solid Films

journal homepage: www.elsevier.com/locate/tsf

Role of Ge nanoclusters in the performance of photodetectors compatible with Si technology

S. Cosentino [a,b,*], S. Mirabella [a], Pei Liu [b], Son T. Le [b], M. Miritello [a], S. Lee [b], I. Crupi [a], G. Nicotra [c], C. Spinella [c], D. Paine [b], A. Terrasi [a], A. Zaslavsky [b], D. Pacifici [b]

[a] MATIS–IMM–CNR and Dipartimento di Fisica ed Astronomia, Università di Catania, Catania I-95123, Italy
[b] School of Engineering, Brown University, Providence RI 02912, USA
[c] IMM–CNR, VIII Strada 8, 95121 Catania, Italy

ARTICLE INFO

Article history:
Received 22 March 2013
Received in revised form 10 September 2013
Accepted 10 September 2013
Available online 17 September 2013

Keywords:
Germanium
Nanocluster
High-efficiency photodetectors
Gain
Response time

ABSTRACT

In this work, we investigate the spectral response of metal-oxide-semiconductor photodetectors based on Ge nanoclusters (NCs) embedded in a silicon dioxide (SiO_2) matrix. The role of Ge NC size and density on the spectral response was evaluated by comparing the performance of PDs based on either densely packed arrays of 2 nm-diameter NCs or a more sparse array of 8 nm-diameter Ge NCs. Our Ge NC photodetectors exhibit a high spectral responsivity in the 500–1000 nm range with internal quantum efficiency of ~700% at −10 V, and with NC array parameters such as NC density and size playing a crucial role in the photoconductive gain and response time. We find that the configuration with a more dispersed array of NCs ensures a faster photoresponse, due to the larger fraction of electrically-active NCs and the partial suppression of recombination centers. The photoconduction mechanism, assisted by trapping of photo-generated holes in Ge NCs, is discussed for different excitation power and applied bias conditions. Our results provide guidelines for further optimization of high-efficiency Ge NC photodetectors.

© 2013 Elsevier B.V. All rights reserved.

1. Introduction

The fabrication of high-performance optoelectronic devices using materials compatible with complementary metal-oxide-semiconductor technology is a current challenge in applied scientific research. Much attention has been devoted to group IV nanostructured materials, such as Si or Ge nanoclusters (NCs), because of the chance to overcome existing limitations of bulk materials due to quantum confinement [1–3]. Compared to Si NCs, Ge NCs reveal interesting properties related to a larger absorption coefficient, a lower E_G and an easier fabrication route due to the lower melting temperature. In addition, the larger exciton Bohr radius of Ge (~24 nm) with respect to Si (~4.9 nm) [4] should allow an easier tuning of the energy gap by varying the NC size. However, to complicate matters, several experimental studies on Ge NCs embedded in a silica matrix showed that their optical properties cannot be explained solely with quantum confinement effects [5–8], as surface effects play a strong role in light absorption/emission mechanisms.

Despite much research into structural and optical properties of Si and Ge NCs in SiO_2, only a few studies have addressed photodetector (PD) devices based on these materials. Only recently, PDs based on silica-embedded Si quantum dots (QDs) showed responsivity up to 2.8 A/W at 1.55 μm and an internal quantum efficiency (IQE) of 200% [9,10], whereas Ge QD-based PDs reached an IQE of ~400% [11,12]. We recently reported on PDs with a ~250 nm active layer of 2 nm-diameter amorphous Ge NCs in SiO_2 with even better performance: very high values of responsivity (up to 4 A/W) and quantum conversion efficiencies up to 700% in the VIS–NIR wavelength range [13]. In addition, this type of PD was demonstrated to achieve a time response down to ~40 ns as the active NCs' layer is thinned to ~60 nm, with minimal loss in responsivity [14].

One open question concerning the use of Ge nanostructures in the fabrication of high-efficiency PDs or light harvesters is whether the structural and absorption properties of such nanostructures can influence the photo-conversion efficiency of the device. In fact, the conduction mechanism of Ge NCs embedded in SiO_2 could strongly depend on the size and separation distance of the NCs, on their amorphous/crystalline structure and on the abundance of defect states at the NC–SiO_2 interface. For this reason, here we present results on two different PDs with active layers consisting respectively of (1) a sparse, random array of crystalline Ge NCs with an average diameter of 8 nm (+/−4 nm), produced after a post-deposition thermal annealing at 800 °C and (2) a densely packed, random array of amorphous Ge NCs with an average diameter of 2 nm (+/−1 nm), as previously reported [13,14]. We find that the average surface-to-surface spacing between NCs and the fraction of electrically-active NCs can strongly influence both the PD efficiency and response time. In particular, a post-thermal annealing at 800 °C of the Ge NC's active layer determines a faster response and, at the same time, a higher photoconductive gain at high reverse bias over a broad spectral range

* Corresponding author at: MATIS–IMM–CNR and Dipartimento di Fisica ed Astronomia, Università di Catania, Catania I-95123, Italy.
E-mail address: salvatore.cosentino@ct.infn.it (S. Cosentino).

0040-6090/$ – see front matter © 2013 Elsevier B.V. All rights reserved.
http://dx.doi.org/10.1016/j.tsf.2013.09.028

(500–1000 nm). These effects can be profitably applied for the potential use of Ge NCs in high-efficiency PDs and light-harvesting devices.

2. Experimental details

Germanium NCs embedded in a silica matrix have been synthesized within a ~250 nm film of Ge-enriched silicon dioxide (SiGeO). The SiGeO film was deposited by rf-magnetron co-sputtering from SiO_2 and Ge targets onto a (100) c-Si n^{-}-type substrate heated at 400 °C [7]. The atomic concentrations of Si, Ge and O were measured by Rutherford backscattering spectrometry (RBS), and were found to be 23%, 18%, and 59%, respectively. Cross-sectional scanning transmission electron microscopy analysis (STEM) showed the presence of small, densely and homogeneously distributed amorphous (a-) Ge NCs in the as-deposited film with a mean diameter of about 2 nm — see Fig. 1(a). Considering the Ge content measured by RBS and the mean size distribution extracted by STEM analysis, we estimate a density of a-Ge NC of ~2×10^{19} cm^{-3}, with a mean NC–NC separation distance <*a*> (estimated surface to surface) of ~1.5 nm, as reported in Table 1. Post-deposition thermal annealing at 800 °C (1 h in N_2 atmosphere) of the as-deposited sample induced the Ostwald ripening growth of larger crystalline (c-) Ge NCs with a mean diameter of about 8 nm, as shown in Fig. 1(b) and in the HRTEM image reported in Fig. 1(c). In this case, a sparse distribution of NCs within the oxide layer is more evident, with a value of <*a*> ~4 nm and a Ge NC concentration of ~6×10^{17} NC/cm^3, see Table 1.

After fabrication of the active layers, metal-oxide-semiconductor PDs (3×3 mm^2 active area) were fabricated by sputter deposition of a transparent conductive indium–zinc-oxide (IZO) thin-film top contact (55 nm thick, 2×10^{-4} Ω-cm resistivity) onto both types of Ge NCs in SiO_2 layers (called from here on: *as-deposited* or *annealed*), whereas the back contact consisted of a silver layer on the back of the *n*-Si wafer. The inset in Fig. 2(a) shows a schematic of the photodetector structure.

Current–voltage *I*(*V*) measurements were performed using an Agilent parameter analyzer 4155C both in dark and under constant illumination with a monochromatized light source spanning the wavelength range at $\lambda = 500$–1000 nm (with a spectral resolution of ~3 nm determined by the spectrograph utilized to disperse the broadband light source). The response time of Ge NCs' PDs was analyzed by illuminating the device (held at constant reverse bias of −2 V or −10 V) with a 960 Hz modulated diode laser at $\lambda = 639$ nm. The photocurrent was measured on a digital oscilloscope by recording the voltage drop across a 2 kΩ resistor in series with the PD.

Table 1
Summary of the SiGeO samples containing Ge NCs deposited on *n*-Si wafer at 400 °C (as-deposited) and post-annealed in N_2 at 800 °C. Ge excess was extracted by RBS measurements while NC mean size was estimated by TEM analysis.

SiGeO sample	As-deposited	Annealed at 800 °C
Mean NC size	2 ± 1 nm	8 ± 4 nm
Ge NCs' concentration	2×10^{19} NC/cm^3	6×10^{17} NC/cm^3
Mean NC–NC distance (surface to surface)	1.5 nm	4 nm

3. Results and discussion

Fig. 2 shows the comparison of *I*(*V*) measurements under reverse bias for the metal-oxide-semiconductor (MOS) PDs with the as-deposited and annealed Ge NC layers, both in the dark and under monochromatic illumination at $\lambda = 500$ and 700 nm, respectively. The dark current is ascribed to electrons tunneling from the IZO reservoir to the n^{-}-Si substrate via a trap-assisted conduction mechanism mediated by the NCs embedded in the SiO_2 matrix [15]. For a low applied bias, we note a slight reduction of the dark current for the PD annealed Ge NCs' layer with respect to the as deposited one. This difference mainly comes from the different NC distribution in the two types of PDs. In fact, after annealing the separation <*a*> between NCs becomes about three times larger, reducing the electron tunneling probability between NCs.

During illumination at 500 and 700 nm there is a clear enhancement of the current with respect to the dark case for both types of PDs, as showed in Fig. 2. This behavior is related to the presence of Ge NCs within the oxide layer, since an analogous MOS PD without Ge NCs does not show any spectral response [13]. We attribute such a large photoresponse to a mechanism of hole-trapping mediated by the Ge NCs [13,14]. According to this model, schematically shown in the inset of Fig. 2, electron-hole pairs (EHP) are photo-generated by the light absorption within the Ge NCs' layer or the Si substrate. Then, the photogenerated holes get preferentially trapped by the Ge NC interface states because of their lower ability to tunnel between NCs into the SiO_2 with respect to electrons. The resulting positive charge localized in the Ge NCs' layer facilitates the extra injection of electrons from the IZO

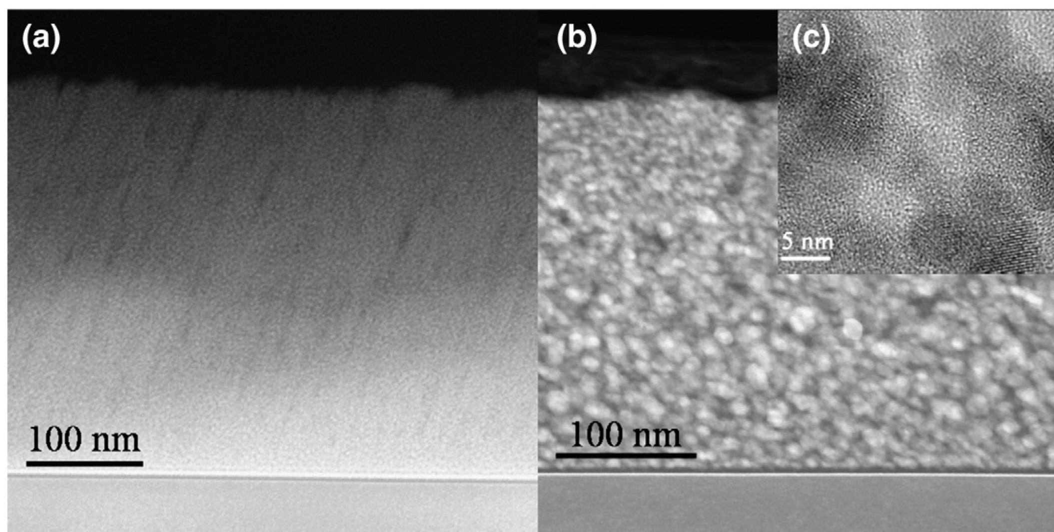

Fig. 1. Cross-sectional dark-field STEM images of the SiGeO sample, as-deposited (a) and after annealing at 800 °C (b). The inset (c) shows a HR-TEM of the annealed sample, revealing the presence of a dense array of crystalline Ge nanoclusters.

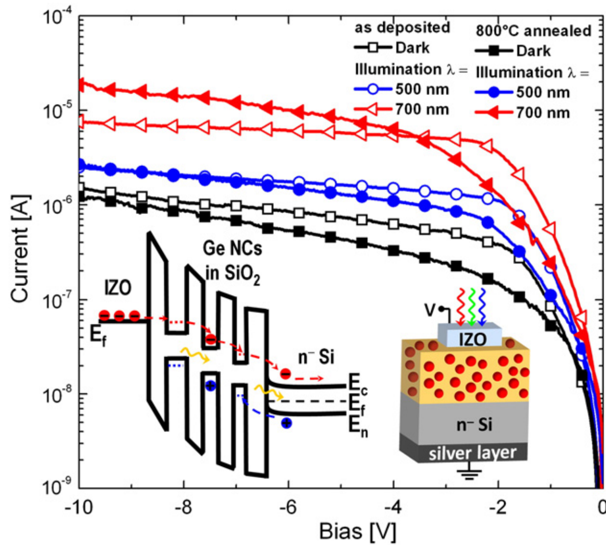

Fig. 2. $I(V)$ characteristics under reverse bias in the dark and under monochromatic illumination for the MOS PD with an as-deposited layer of densely packed, 2 nm-diameter a-Ge NCs (open symbols) or an annealed layer of sparse, 8 nm-diameter c-Ge NCs (closed symbols). Insets show a schematic of the photodetector structure and the mechanism of conduction in Ge NCs' PDs under bias and illumination.

contact, giving rise to high currents under illumination. This model also agrees with the long hole-retention time reported by Sousa et al. for $Si_{1-x}Ge_x$ NC-based memories and with the results reported by Zhang et al., who showed high *p*-type conductivity in thin films composed of Ge NCs in SiO_2 attributable to hole trapping at the Ge NC surface states [16,17].

In addition, we can distinguish two different regimes of the photocurrent with respect to the applied bias. For $-2 < V < 0$ the photocurrent exhibits a strong bias dependence for both types of PDs, while for larger values of the applied bias the photocurrent saturates. This behavior can be explained by a non-uniform electric field distribution across the NC layer and it is typical in superlattice-based devices [18,19]. For low values of the applied bias, we can consider the electric field E mostly uniformly distributed across the Ge NCs' layer and the current increases with bias because of the increasing of electron tunneling probability between NCs. For higher values of V a nonlinear distribution of the E-field takes place, due to the preferential charging of NCs near the Si interface by hole trapping. This effect leads to the formation of a high E-field domain across the neutral NCs and a low uniform electric field region across the rest of NCs' layer because the total applied bias remains constant (as schematized in the band diagram in the inset of Fig. 2). Therefore, any further increase of the applied bias will mainly result in an increase of the E-field only in the high E-field domain region, leading to the saturation of the overall current with respect to the applied bias.

For a more quantitative analysis of the spectral response and conduction mechanism properties of our PDs, we turn our attention to the spectral responsivity, R_{sp}, defined as the photocurrent produced by the device at a given power and wavelength of the incident light:

$$R_{sp}(\lambda) = \frac{\left(I_{\text{light}} - I_{\text{dark}}\right)}{P_{ph}(\lambda)} \quad (1)$$

where the quantity in the numerator is the net photocurrent under illumination for a given voltage, while $P_{ph}(\lambda)$ is the spectral distribution of the incident photon power, determined using a calibrated Si photodetector. Fig. 3(a) compares the spectral responsivity of both types of PDs at two different values of applied bias, $V = -10$ V and -2 V. At -10 V, both devices exhibit high values of responsivity in a broad range of wavelengths from 500 to 1000 nm. The responsivity peaks at

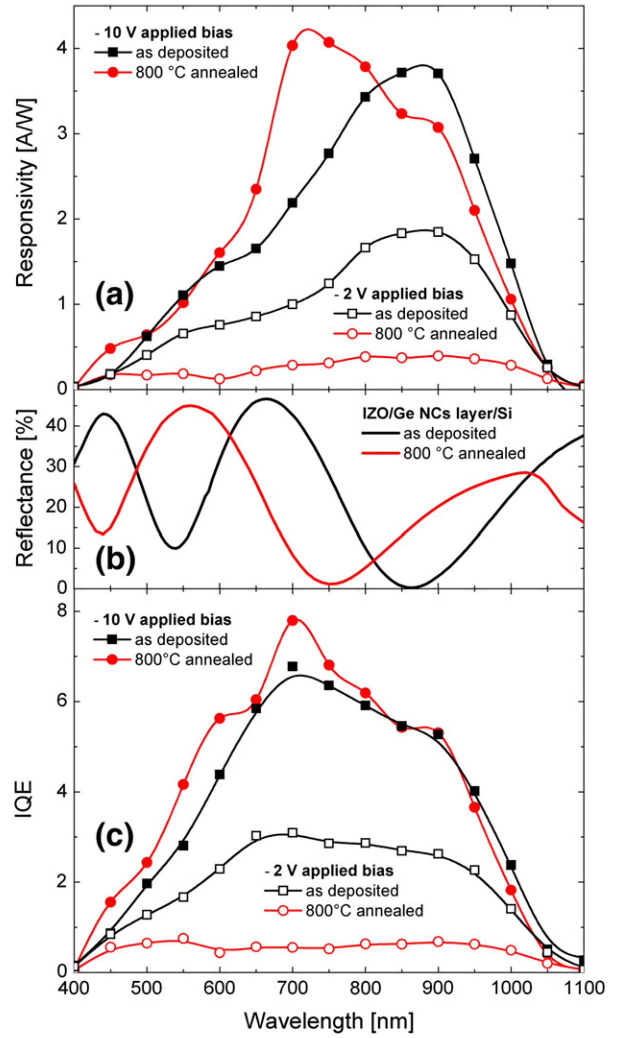

Fig. 3. Comparison between the spectral responsivity R_{sp} (a), reflectance (b) and IQE spectra (c) of MOS PDs with an as-deposited layer of 2 nm-diameter closely packed a-Ge NCs or an annealed layer of 8 nm-diameter dispersed c-Ge NCs.

different λ for the two types of NCs because of a wavelength shift in the reflectance minima observed in the specular reflectance spectra, determined by a densification and structural change of the active layer upon annealing (as reported in Fig. 3(b)). However, in both devices the responsivity approaches a value of 4 A/W, moreover, as discussed below, the internal quantum efficiency shows remarkably similar spectral features when reflectance is divided out (see Fig. 3(c) and detailed discussion in the following). On the other hand, at $V = -2$ V, the PD with the as-deposited, densely-spaced array of Ge NCs exhibits much higher responsivity than the annealed one.

To better clarify the role of Ge NCs in the conduction mechanism of this device, it is essential to relate the absorption properties to the current behavior during illumination. To this end, we calculated the spectral IQE, defined as the number of carriers collected at the output of the device per each absorbed photon at a given voltage.

$$\text{IQE} = \frac{hc}{\lambda} \cdot \frac{\left(I_{\text{light}} - I_{\text{dark}}\right)}{(1-R) \cdot P_{ph}} \quad (2)$$

where R is the reflectance of our Ge NCs' MOS PDs, measured using a calibrated Si standard reference and shown in Fig. 3(b).

Results of IQE are shown in Fig. 3(c). For both the as-deposited or annealed Ge NCs' arrays, we find IQE values higher than 100% in the 500–1000 nm range at a bias of −10 V, with a remarkably similar spectral response with a maximum of ~700% at 700 nm. Thus, the larger separation distance between NCs after thermal annealing does not seem to significantly affect the high photoconductive gain achieved by this type of PDs under high reverse bias (−10 V). However, for a lower applied bias of −2 V, the PD with as-deposited and densely packed Ge NCs still exhibits a large photoconductive gain in the 500–1000 nm range, approaching a maximum value of ~300% at 700 nm, whereas the annealed device is characterized by an IQE of only ~60%. This behavior is attributable to the easier hopping conduction of carriers occurring in the denser array of Ge NCs embedded in SiO_2 in the low bias regime. The increased spacing between Ge NCs after annealing at 800 °C strongly reduces the tunneling probability and, consequently, the device IQE at low applied bias as observed in Fig. 3(c). Moreover, it is important to observe that both MOS PDs with small (densely packed) and large (sparse) Ge NCs show very broad wavelength responsivity, indeed broader than the light absorption range of Ge NCs. Fig. 4 shows the fraction of incident light absorbed by our samples, calculated using the absorption coefficient obtained from reflectance and transmittance measurements [7]. If the optical bandgap in Ge NCs was determined by quantum size confinement only, smaller NCs would be expected to absorb at much shorter wavelengths. According to the analysis by Barbagiovanni et al., for 2 nm Ge NCs we should expect an optical onset at λ ~ 800 nm, whereas the large 8 nm Ge NCs should absorb at λ ~ 1700 nm, very close to the bulk regime [20]. However, experimentally we find that both sizes of our Ge NCs are optically active only for wavelengths at λ < 800 nm, since they exhibit an optical bandgap pinned at ~1.6 eV by surface state effects that mask the quantum confinement regime [7]. Because of this, the spectral response of our PDs does not shift with the NC size, as observed in Fig. 3(c). Moreover, the high photoconductive gain cannot be explained by the direct photo-carrier generation in the Ge NC layer alone, as there is also a non-negligible contribution of photo-carriers coming from the Si substrate. In particular, for λ < 800 nm the photogeneration of holes is due to the absorption of light both by the Ge NCs and the Si substrate (with the NC absorption dominant at smaller wavelengths). So, for λ < 800 nm, the Ge NCs play two roles: they act as hole-photo-generation (1) and hole-trapping (2) centers. For λ > 800 nm Ge NCs are mostly transparent to the incident light, which can therefore be absorbed only by the Si substrate (see Fig. 4). In this case, the main role of Ge NCs is to trap photo-generated holes injected from the Si substrate and act as a hopping conduction channel for the electrons injected from the IZO gate contact. Therefore, the contribution of the Si substrate in the photo-generation of holes is crucial to explain the observed gain in our PDs, especially for wavelengths where Ge NCs do not play a significant role in the optical absorption of incident photons.

To test the electrical activation of the Ge NCs by hole trapping and the response time after light illumination, we performed time-resolved photocurrent $I(t)$ measurements at −2 V and −10 V by illuminating our PDs with a chopped laser at $\lambda = 639$ nm. From $I(t)$ measurements we can define the switching time, t_{on}, as the time needed by the photocurrent to reach a value of $(1–1/e)$ of its maximum after illumination. The t_{on} is linked both to the electrical activation time of NCs by hole trapping and to the transit time of the injected electrons from the IZO gate through the activated NCs' channel. In Fig. 5(a) we report the photocurrent rise time (normalized to the peak value) for low (15 μW) and high (1 mW) excitation power at $V = -2$ V. For both types of PDs, we observe a clear power dependence of t_{on} which decreases with increasing incident power, in agreement with a larger number of NCs being electrically activated by trapping of photo-generated holes. In particular, the t_{on} of the PD with as-deposited 2 nm Ge NCs goes from ~2 μs to

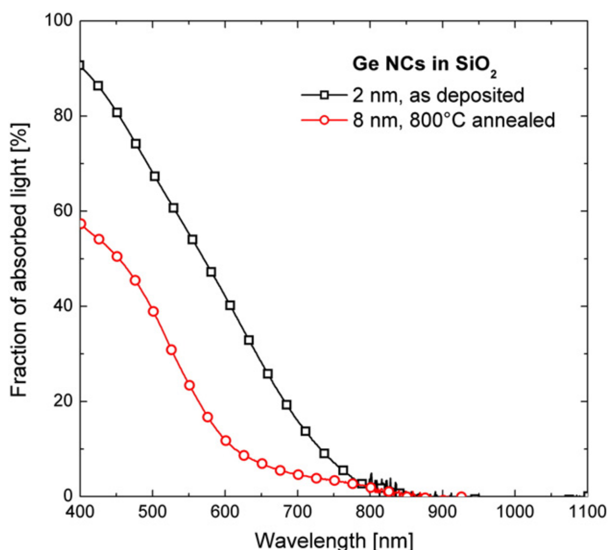

Fig. 4. Fraction of the light absorbed by a 250 nm thick SiGeO layer with a-Ge NCs of 2 nm or c-Ge NCs of 8 nm diameter.

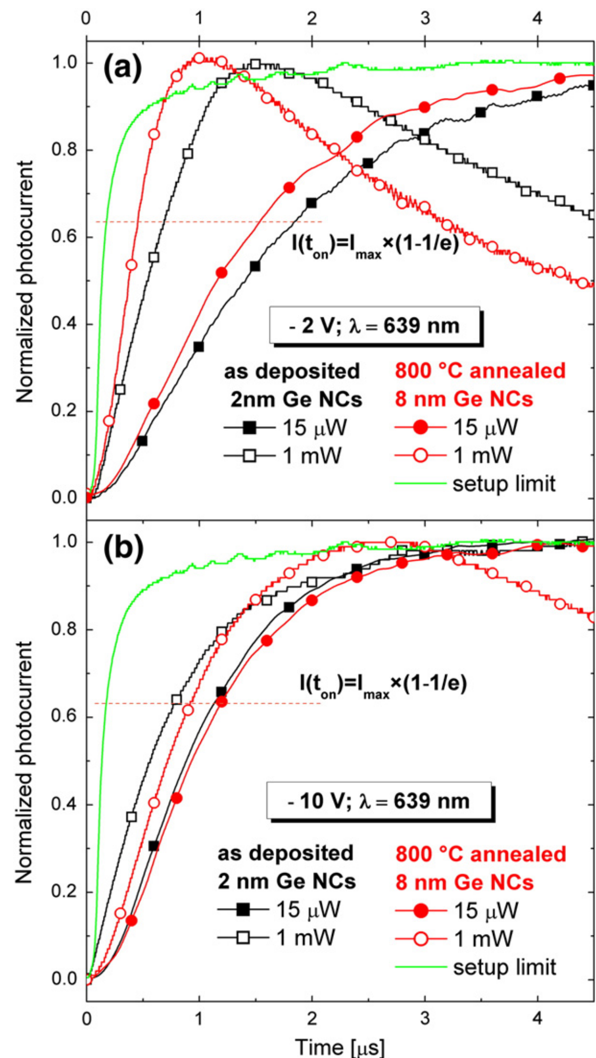

Fig. 5. Normalized photocurrent response time curves of MOS PDs with an as-deposited layer of closely-spaced, 2 nm-diameter a-Ge NCs (squares) or an annealed layer of sparse, 8 nm-diameter c-Ge NCs (circles) at −2 V (a) and −10 V (b) for low (15 μW, closed symbols) and high (1 mW, open symbols) excitation power. The continuous green line represents the baseline system response (~0.1 μs response time) obtained by measuring the modulated laser beam using a commercial Si photodiode with nanosecond response time.

~0.65 μs as the incident power is increased from 15 μW to 1 mW. For the same incident powers, the PD with 8 nm crystalline Ge NCs exhibits a faster response to the incident light, with a t_{on} going from about ~1.5 μs to ~0.45 μs. In this case, a larger fraction of NCs is activated by hole trapping, since the Ge NCs' concentration only becomes 3% of the value of the as-deposited sample after annealing at 800 °C (Table 1). Thus, a faster conduction via percolative hopping through the electrically-activated NCs is possible for the electrons coming from IZO. In this regard, the amorphous to crystalline structural transition of Ge NCs after the annealing at 800 °C can contribute to a faster response time, due to the reduction of defects surrounding the NC–SiO_2 interface that act as recombination centers for EHP. Fig. 5(b) shows the comparison between the response time of our PDs at $V = -10$ V, which is around 1 μs, and decreases only slightly when the excitation power is increased. In this case, the different size and density of NCs does not affect the response time significantly. At 1 mW both types of PDs exhibit a slower response time with respect to the −2 V case. This behavior can be related to the different conduction regime occurring at high values of the applied bias and also responsible of the photocurrent saturation discussed above in Fig. 2. In particular, for high excitation powers a larger fraction of Ge NCs are preferentially charged near the Si interface by photo-induced hole trapping. This effect leads to an additional non-linear distribution of the electric field E that further lowers the average field across the charged NC layer and reduces the hopping rate of carriers between NCs, causing a slower response time.

In conclusion, our results indicate that the structural properties of Ge NCs such as size, NC density and separation distance and NC structural phase, can strongly influence the efficiency and response time performances of this type of PDs. In particular, we compared the photoresponse of two PDs with different active layers consisting respectively of (1) a randomly distributed array of densely packed (surface-to-surface separation $\langle a \rangle$ ~1.5 nm) amorphous Ge NCs with a mean diameter of 2 nm, and (2) a randomly distributed array of more sparse ($\langle a \rangle$ ~4 nm) crystalline Ge NCs with a mean diameter of 8 nm, both embedded in an amorphous matrix of SiO_2. The PD with closely packed Ge NCs shows a very high photoconductive gain (~300%) even for a low applied bias of −2 V due to higher tunneling probability, but a slower response time due to the presence of recombination centers for EHP at the NC/SiO_2 interface and by the high concentration of NCs that need to be activated in order to contribute to an efficient conduction mechanism. The PD with a more dispersed array of 8 nm Ge NCs still shows a high photoconductive gain (~700%) at −10 V, because of the efficient tunneling probability at high bias and the larger fraction of activated NCs responsible of the gain mechanism. This PD also exhibits a faster response time at low bias (~0.45 μs at 1 mW) due to the larger fraction of electrically-active NCs and the lower amount of recombination centers compared to the 2 nm amorphous Ge NCs' PD. This feature is very promising since the response time could be further improved by orders of magnitude by simply thinning the NC layer, as already demonstrated for 2 nm-diameter Ge NCs' PD [14]. The results reported in this paper can lead to optimized design strategies for faster and higher efficiency photodetectors based on Ge NCs.

Acknowledgments

This work was performed at Brown University and at the University of Catania. The work at Brown University was funded by the National Science Foundation (NSF Grant No. DMR-1203186). The research activity of S. Cosentino was supported by a scholarship grant of Blanceflor Boncompagni-Ludovisi foundation.

References

[1] L. Pavesi, L. Dal Negro, C. Mazzoleni, G. Franzò, F. Priolo, Nature 408 (2000) 440.
[2] G. Conibeer, Mater. Today 10 (2007) 11.
[3] S. Mirabella, R. Agosta, G. Franzò, I. Crupi, M. Miritello, R. Lo Savio, M.A. Di Stefano, S. Di Marco, F. Simone, A. Terrasi, J. Appl. Phys. 106 (2009) 103505.
[4] A.G. Cullis, L.T. Canham, P.D.J. Calcott, J. Appl. Phys. 82 (1997) 909.
[5] Y. Maeda, Phys. Rev. B 51 (1995) 1658.
[6] M. Fuji, O. Mamezaki, S. Hayashi, K. Yamamoto, J. Appl. Phys. 83 (1998) 1507.
[7] S. Cosentino, S. Mirabella, M. Miritello, G. Nicotra, R. Lo Savio, F. Simone, C. Spinella, A. Terrasi, Nanoscale Res. Lett. 6 (2011) 135.
[8] C. Uhrenfeldt, J. Chevallier, A.N. Larsen, B.B. Nielsen, J. Appl. Phys. 109 (2011) 094314.
[9] J.M. Shieh, W.C. Yu, J.Y. Huang, C.K. Wang, B.T. Dai, H.Y. Jhan, C.W. Hsu, H.C. Kuo, F.L. Yang, C.L. Pan, Appl. Phys. Lett. 94 (2009) 241108.
[10] J.M. Shieh, Y.F. Lai, W.X. Ni, H.C. Kuo, C.Y. Fang, J.Y. Huang, C.L. Pan, Appl. Phys. Lett. 90 (2007) 051105.
[11] S.S. Tzeng, P.W. Li, Nanotechnology 19 (2008) 235203.
[12] S.S. Tseng, I.H. Chen, P.W. Li, Appl. Phys. Lett. 93 (2008) 191112.
[13] S. Cosentino, Pei Liu, Son T. Le, S. Lee, D. Paine, A. Zaslavsky, D. Pacifici, S. Mirabella, M. Miritello, I. Crupi, A. Terrasi, Appl. Phys. Lett. 98 (2011) 221107.
[14] Pei Liu, S. Cosentino, Son T. Le, S. Lee, D. Paine, A. Zaslavsky, D. Pacifici, S. Mirabella, M. Miritello, I. Crupi, A. Terrasi, J. Appl. Phys. 112 (2012) 083103.
[15] A.I. Chou, K. Lai, K. Kumar, P. Chowdhury, J.C. Lee, Appl. Phys. Lett. 70 (1997) 3407.
[16] J.S. de Sousa, V.N. Freire, J.-P. Leburton, Appl. Phys. Lett. 90 (2007) 223504.
[17] B. Zhang, S. Shrestha, M.A. Green, G. Conibeer, Appl. Phys. Lett. 97 (2010) 132109.
[18] M. Ershov, V. Ryzhii, C. Hamaguchi, Appl. Phys. Lett. 67 (1995) 3147.
[19] V. Letov, M. Ershov, S.G. Matsik, A.G.U. Perera, H.C. Liu, Z.R. Wasilewski, M. Buchanan, Appl. Phys. Lett. 79 (2001) 2094.
[20] E.G. Barbagiovanni, D.J. Lockwood, P.J. Simpson, L.V. Goncharova, J. Appl. Phys. 111 (2012) 034307.